JOURNAL OF NEUROTRAUMA 30:907–919 (June 1, 2013)

DOI: 10.1089/neu.2012.2657

Original Articles

Remote Brain Network Changes after Unilateral Cortical Impact Injury and Their Modulation by Acetylcholinesterase Inhibition

Daniel P. Holschneider,[1–5] Yumei Guo,[1] Zhuo Wang,[1] Margareth Roch,[5] and Oscar U. Scremin[5,6]

Abstract

We explored whether cerebral cortical impact injury (CCI) effects extend beyond direct lesion sites to affect remote brain networks, and whether acetylcholinesterase (AChE) inhibition elicits discrete changes in functional activation of motor circuits following CCI. Adult male rats underwent unilateral motor-sensory CCI or sham injury. Physostigmine (AChE inhibitor) or saline were administered subcutaneously continuously via implanted minipumps (1.6 micromoles/kg/day) for 3 weeks, followed by cerebral perfusion mapping during treadmill walking using [^{14}C]-iodoantipyrine. Quantitative autoradiographs were analyzed by statistical parametric mapping and functional connectivity (FC) analysis. CCI resulted in functional deficits in the ipsilesional basal ganglia, with increased activation contralesionally. Recruitment was also observed, especially contralesionally, of the red nucleus, superior colliculus, pedunculopontine tegmental nucleus, thalamus (ventrolateral n., central medial n.), cerebellum, and sensory cortex. FC decreased significantly within ipsi- and contralesional motor circuits and between hemispheres, but increased between midline cerebellum and select regions of the basal ganglia within each hemisphere. Physostigmine significantly increased functional brain activation in the cerebellar thalamocortical pathway (midline cerebellum → ventrolateral thalamus → motor cortex), subthalamic nucleus/zona incerta, and red nucleus and bilateral sensory cortex. In conclusion, CCI resulted in increased functional recruitment of contralesional motor cortex and bilateral subcortical motor regions, as well as recruitment of the cerebellar–thalamocortical circuit and contralesional sensory cortex. This phenomenon, augmented by physostigmine, may partially compensate motor deficits. FC decreased inter-hemispherically and in negative, but not positive, intra-hemispherical FC, and it was not affected by physostigmine. Circuit-based approaches into functional brain reorganization may inform future behavioral or molecular strategies to augment targeted neurorehabilitation.

Key words: cholinergic; diaschisis; functional brain mapping; functional connectivity; traumatic brain injury

Introduction

Motor impairments are a frequent finding after traumatic brain injury (TBI).[1–4] Brain-injured patients may show persistent impairments across multiple functions and behaviors, the profile of which does not always correspond to the size and location of injuries. One possible explanation is that TBI-induced damage extends beyond initial lesion sites to affect brain networks at a distance (''diaschisis'').[5] In addition, compensatory strategies may be engaged in response to functional deficits that 'recruit' brain regions in a manner unlike that observed in normal subjects. Compensatory strategies of the lesioned brain to reduce motor deficits have centered on: (1) increased reliance on residual, non-lesioned neurons in the affected motor circuits; (2) transfer of function to other types of neurons in the affected motor circuits; (3) increased reliance on contralateral circuits (stroke),[6–9] (TBI);[10] and (4) learning of alternate behavioral strategies for executing a given task, with transfer of function to alternate motor and sensory circuits (reviewed in Refs. 11 and 12). Such compensatory strategies may augment or impede motor recovery but are lacking a sound scientific understanding.[8,9]

In the current study, we use a rat model to explore functional reorganization of the motor circuit following unilateral motor-sensory cortical injury. Despite their differences, remarkable similarities exist between the rat model and humans at the level of the anatomy of motor circuits, the general distribution of chemical markers of striatal and pallidal structures, as well as similarities in development and motor processing.[13–16] Treadmill walking in

[1]Departments of Psychiatry and the Behavioral Sciences, Keck School of Medicine at University of Southern California, Los Angeles, California. Departments of [2]Neurology, [3]Biomedical Engineering, [4]Cell and Neurobiology, University of Southern California, Los Angeles, California.
[5]Research Service, Veterans Affairs Greater Los Angeles Healthcare System, Los Angeles, California.
[6]Physiology Department, David Geffen School of Medicine at UCLA, Los Angeles, California.

normal rats[17,18] has shown that this task activates equivalent motor circuits to those activated in humans[19,20] Likewise, the way rats use forelimbs to reach and grasp objects has been found to have major homologies with human reaching.[21–23] This conservation of supraspinal networks between rats and humans provides a close animal-to-human translation of the proposed circuit-based neuroimaging approach to functional brain reorganization. In the work outlined below, we apply cerebral perfusion mapping in the rat model during a locomotor challenge to provide a detailed map of regional changes in functional brain activation. In addition, we apply interregional correlation-based functional connectivity analysis to explore how lesions affect brain activity at the network level.[24–26] Finally, because recent work by our group showed that low dose, subchronic administration of physostigmine following TBI may improve components of motor function,[27] we now examine if physostigmine elicits discrete changes in the functional activation of motor circuits following motor-sensory cortical impact injury (CCI).

Methods

Animals

Forty-three Sprague-Dawley male rats (250–300 g body mass, Harlan Sprague Dawley, Placentia, CA) were used. Twenty of them received TBI, and 23 received a sham intervention, as described below. TBI animals were divided into two groups receiving continuous subcutaneous infusion of saline (Lesion/Saline, $n=11$) or physostigmine (Lesion/Phy, $n=9$, 1.6 μmoles/kg/day). Matching groups were set up for sham intervention rats that received saline (Sham/Saline, $n=14$), or physostigmine (Sham/Phy, $n=9$). The research environment and protocol for animal experimentation were approved by the Institutional Animal Care and Use Committee (IACUC) of the West Los Angeles Veterans Affairs Healthcare System and the USC School of Medicine. The animal facilities at these institutions are accredited by the Association for Assessment and Accreditation of Laboratory Animal Care (AAALAC), International. Animals were group housed during a 1-week period of acclimatization to the vivarium prior to experimentation. Rats were individually housed following surgery, with free access to water and standard rodent chow for the duration of the study.

Controlled cortical impact (CCI)

Rats were anesthetized with isoflurane (induction 3.5%, maintenance 2.0%). Trauma of the right cerebral cortex was produced with a modification of the method of Allen[28] and Feeney et al.[29] Methods were identical to those reported previously.[27,30] In brief, following sterile technique, a right parasagittal skin incision was performed, the galea incised and reflected and a craniotomy fashioned, with a 6.2 mm trephine, centered at 1.2 mm anterior and 3.5 mm lateral (right side) to bregma. A 20 g weight was dropped through a vented stainless steel guide tube from a height of 35 cm to strike a stainless steel circular, flat footplate (4.5 mm diameter) resting on the exposed dura mater of the right motor-sensory cortex, with its center 1.2 mm anterior and 3.5 mm lateral to bregma ($\sim$AP 3.4 mm to -1.0 mm, Lat 5.7 mm to 1.3 mm). This site was selected to coincide with the maximum activation of the primary motor cortex observed in rats during treadmill walking.[17] The indentation produced in the cortex by the footplate was limited to 3.0 mm. Sham intervention animals were anesthetized as described above, skin and galea incisions were made and then sutured, but no craniotomy and cortical impact were produced. Animals were provided a source of heat to prevent post-operative hypothermia. Antibiotic (Cefazolin-Na, 100 mg/kg i.m.) and analgesic therapy (flunixin meglumine, 1.1 mg/kg, s.c.), twice daily, was maintained during 3 days after TBI or Sham interventions.

Administration of physostigmine hemisulfate

Physostigmine hemisulfate (Sigma Aldrich, St. Louis, MO) and ethylenediaminetetraacetic acid disodium salt dehydrate (EDTA, Sigma Aldrich) were dissolved at equimolar concentrations in double distilled boiled water, and 2 mL of the solution were used to fill each osmotic pump (Alzet Model 2ML4, Durect Corp. Cupertino, CA). The pumps are cylindrical in shape, with a length of 3 cm, a diameter of 0.7 cm, a weight of 1.1 grams empty, and deliver 2.5 μL/h continuously during 21 days. They were inserted into a subcutaneous space created by blunt dissection of the interscapular region of animals under isoflurane anesthesia. The skin was closed with 2-0 prolene sutures. The molar infusion rate of the acetylcholinesterase inhibitor was 1.6 μmoles/kg/day. Drug delivery was confirmed on explantation of the pump at the end of the experiment by aspiration of the remaining drug, as well as weighing of the pumps. At the physostigmine infusion rates of 1.6 μmoles/kg/day, no signs of cholinergic toxicity were observed at any time. We have previously shown that this physostigmine dose following 3 weeks of infusion reduces cortical acetylcholinesterase activity to 91%–95% of control and improves performance in the accelerating Rotarod paradigm.[27] Earlier work using [^{3}H]-physostigmine showed that its distribution is across the entire brain, and that the cerebral concentration of [^{3}H]-physostigmine is correlated with the regional cerebral blood flow (rCBF) during the uptake phase of intravenous pulse administration.[31] This flow-dependent characteristic ensures that the areas that are activated during a task (i.e., with increased rCBF) will receive the greatest relative amount of physostigmine when it is administered continuously, as in the present experiments.

Functional brain imaging

Seventeen days after TBI, animals were anesthetized (isoflurane 1.5% maintenance) and implanted using sterile technique with external jugular vein catheters (3.5-Fr. silastic) with the tip advanced into the superior vena cava. The distal end of the catheter was tunneled subcutaneously from the ventromedial aspect of the neck to the infrascapular region, externalized, and then capped with a stainless steel plug. Catheters were flushed every other day with (0.8 mL of 4 U heparin/mL in 0.9% saline, followed by 0.1 mL of a lock solution of 20 U/mL heparin in 0.9% saline).

Brain mapping was conducted 4 days after catheter implantation between noon and 5 PM under standard laboratory lighting conditions with a background noise level of 60 dB. Brain mapping was performed during a Rotarod locomotor challenge, which our prior work in nonlesioned rats showed results in functional activation of the classical basal ganglia circuit, as well as midline cerebellum.[18] This task activates equivalent motor circuits to those activated in humans during treadmill walking.[19,20] Rats were placed in a metal transport cage with a wire mesh top and habituated for 30 min to the experimental room. The Rotarod spindle (7.3 cm diameter) and transport cage were wiped with a cloth dampened with 1% ammonia between animals to minimize olfactory cues. Novelty effects were minimized due to prior exposure of the rats to both the Rotarod and the transport cage. At the start of the experiment, animals were refamiliarized with treadmill walking on the Rotarod for 2 min at 8 rpm (3.1 cm/sec). Thereafter, the rats were removed and the percutaneous port was quickly connected to an external catheter loaded on one end with 125 μCi/kg of [^{14}C]-iodoantipyrine (American Radiolabelled Chemicals, MO) in 300 μL of 0.9% saline, and to a syringe filled with euthanasia agent (pentobarbital 75 mg/kg, 3 M potassium chloride) on the other. Rats were then returned to slow walking on the Rotarod at a speed of 8 rpm. The catheter was loosely supported over the Rotarod, with the syringe placed into a mechanical infusion pump placed behind the Rotarod.

Injection of the tracer occurred by motorized pump at 2.25 mL/min after 2 min of treadmill walking. Immediately after bolus injection of the tracer, the euthanasia solution was injected into the

circulatory system. This resulted in cardiac arrest within ~8–10 seconds, a precipitous fall of arterial blood pressure, termination of brain perfusion, and death. This 8–10 second time window provides the temporal resolution during which the distribution of regional cerebral blood flow-related tissue radioactivity was mapped.[32] Regional cerebral blood flow (rCBF) was measured by the classic [^{14}C]-iodoantipyrine method.[33–35] In this method, there is a strict linear proportionality between tissue radioactivity and rCBF when the radioactivity data is captured within a brief interval (~10 sec) after the radiotracer injection.[36,37]

Brains were rapidly removed, flash frozen in dry ice/methylbutane (−55°C), embedded in OCT^{TM} compound (Miles Inc., Elkhart, IN), and stored in a freezer at −0°C. Brains were subsequently cut in a cryostat at −18°C in 20-μm-thick coronal sections with a 300 μm interslice distance. Sections were heat-dried on glass slides and exposed for 2 weeks at room temperature to Kodak Biomax MR film in spring-loaded x-ray cassettes along with 16 radioactive ^{14}C standards (Amersham Biosciences, Piscataway, NJ). Autoradiographs were placed on a voltage stabilized light box (Northern Lights Illuminator, InterFocus Ltd, England), imaged with a Retiga 4000R charge-coupled device monochrome camera (Qimaging, Canada) and a 60 mm Micro-Nikkor macro lens (Nikon, USA), digitized on an 8-bit gray scale using Qcapture Pro 5.1 (Qimaging, Canada) using an ATI FireGL V3100 128 MB digitizing board on a microcomputer. Spatial resolution for the detection of changes in rCBF was 100 μm.[38]

Image analysis

Fifty-seven digitized serial coronal sections were selected and stored as two-dimensional arrays of 40 μm^2 pixels. Adjacent sections were aligned both manually and using TurboReg, an automated pixel-based registration algorithm[39] that sequentially registered each section to the previous section. The aligned sections were imported as an image stack using ImageJ (NIH, Bethesda, MD—http://rsb.info.nih.gov/ij/) with final voxel dimensions of $0.040 \times 0.040 \times 0.3$ mm^3. All brains were smoothed with a Gaussian kernel (FWHM = 3 times the voxel dimensions). Individual 3D images were spatially normalized into a standard space defined by a template of the rat brain. To preserve the shapes of the sections, we used a nonwarping geometric model that included rotations and translations (rigid-body transformation), and used nearest-neighbor interpolation. Details can be found in our publication.[18] We employed cost function masking for the spatial normalization of the lesioned brain. Binary masks were created of the lesioned areas in each TBI animal by manually depicting the precise boundaries of any gross lesions directly on the autoradiographic images using the MRIcron software (http://www.cabiatl.com/ mricro/mricron/index.html).[40,41] Lesion volume was calculated across serial coronal sections using the 300 μm interslice distance. Signal under the masked area in each animal was removed from the calculation of the transformations needed to normalize the image in order to avoid distortion.

SPM analysis. Statistical Parametric Mapping (SPM) (http://www.fil.ion.ucl.ac.uk/spm/)[42,43] was developed for analysis of imaging data in humans and has been adapted by us for use in rat brain autoradiographs[18] and as confirmed by others.[44,45] Global differences in the absolute amount of radiotracer delivered to the brain were adjusted by the SPM software in each animal by scaling the voxel intensities so that the mean intensity for each brain was the same (proportional scaling). Voxels for each brain failing to reach a specified threshold (80%) were masked out to eliminate the background and ventricular spaces.

Unbiased, voxel-by-voxel, between-group statistical analyses were performed in SPM to identify significant task-related changes in functional brain activation. We first ran a factorial analysis, equivalent to running an ANOVA test at each voxel, to identify rCBF changes reflecting main effects of lesion, drug, and lesion x drug interaction. To further delineate direction of those rCBF changes, we performed between-group Student's *t*-test. Statistical significance was established at the voxel level ($p < 0.05$) with minimum cluster extent of 100 contiguous voxels. Brain regions were identified using coronal, sagittal, and transverse views according to the rat brain atlas.[46] Group subcortical differences in the distribution of CBF-TR were displayed as color-coded statistical parametric maps superimposed on the brain coronal slices.

Region-of-interest definition. Regions of interest (ROIs) were defined and data extracted as follows. Clusters showing significant main effects of lesion or drug or lesion x drug interaction in the SPM factorial analysis ($p < 0.05$, extent threshold > 100 contiguous voxels) were combined through logical disjunction to create a master cluster. Anatomical ROIs were then drawn manually in MRIcro (version 1.40, http://cnl.web.arizona.edu/mricro.htm) for each hemisphere of the template brain according to the rat brain atlas. A total of 31 anatomic ROIs were selected, representing the basal ganglia-thalamocortical circuit, the cerebellar thalamocortical circuit, and associated motor regions as defined in Figure 3. Manually drawn ROIs were then combined with this master cluster through logical conjunction to create functional ROIs representing discrete anatomic regions showing task-related functional activation as previously described.[47] Mean optical density of each functional ROI was extracted for each animal using the Marsbar toolbox for SPM (version 0.42, http://marsbar.sourceforge.net/).

Pairwise interregional correlation analysis. We applied inter-regional correlation analysis to investigate functional connectivity. This is a well-established method, which has been applied to analyze rodent brain mapping data of multiple modalities, including autoradiographic deoxyglucose uptake,[48–50] autoradiographic CBF,[47,51] cytochrome oxydase histochemistry,[52–54] and fMRI.[55] In these studies, correlations are calculated in an *inter*-subject manner (i.e., across subjects within a group and different from the *intra*-subject cross correlation analysis often used on fMRI time series data).[56–59] An inter-regional correlation matrix was calculated across animals for each group in Matlab (version 6.5.1, The MathWorks, Inc., Natick, MA, USA). The matrices were visualized as heatmaps with Z-scores of Pearson's correlation coefficients color-coded. Statistical significance of between-group difference of a correlation coefficient was evaluated using the Fisher's Z-transform test ($p < 0.05$).

Seed analysis. Given the prominent compensatory increases in functional activation of contralesional anterior primary motor cortex in the lesioned animals, we used SPM to evaluate significant correlation in rCBF ($p < 0.05$, extent threshold > 100 contiguous voxels) for this brain region across the whole brain in each group of animals. Significant correlations were interpreted as functional connection and displayed as color-coded statistical parametric maps superimposed on the brain coronal slices.

Results

Lesioning resulted in a lesion volume of 12.6 ± 3.3 mm^3 in the saline-treated animals, and a lesion volume of 10.3 ± 2.8 mm^3 in the physostigmine-treated animals, with no significant group difference.

Effects of lesion on motor circuits

Factorial analysis. Significant main effects are summarized in Table 1. Significant effects of lesion on functional brain activation were noted across the motor circuit ipsilesionally and more

Table 1. Brain Regions within the Motor Circuit Showing Significant Main Effects and Interaction in Factorial Analysis

	Lesion		*Drug*		*Lesion x Drug*	
	contra	*ipsi*	*contra*	*ipsi*	*contra*	*ipsi*
Motor cortex, primary (M1)	*	*			*	
secondary (M2)	*	*	*		*	*
Striatum, dorsolateral (dl-CPu)	*	*		*		*
Globus pallidus, internal (GPI)		*	*	*	*	*
external (GPE)					*	*
Substantia nigra (SN)			*	*		
Subthalamic n./zona incerta (STN/ZI)	*	*			*	*
Thalamus, ventrolateral (VL)	*					*
ventromedial (VM)	*					*
central medial n. (CM)	*					
Pedunculopontine tegmental nucleus (PPN)	*					
Superior colliculus (SC)	*	*	*	*		
Red nucleus (RPC)	*					
Cerebellum, vermis	*		*		*	
intermediate lobule (SimA)	*				*	*
medial n. (medCb)	*					

Significant effects for 'Lesion', 'Drug', and 'Lesion x Drug' are depicted for regions ipsilateral (ipsi) and contralateral (contra) to the lesion (*$p < 0.05$).

broadly contralesionally. Ipsilesional changes were significant primarily at the level of motor cortex (primary and secondary), the dorsolateral striatum, the internal globus pallidus, subthalamic nucleus/zona incerta region, and the superior colliculus. Contralesionally, significant changes included the above regions, as well as the thalamus (ventrolateral, ventromedial), the red nucleus, the pedunculopontine tegmental nucleus, as well as medially in the central medial thalamus. In addition, lesions resulted in significant changes in rCBF in the cerebellar vermis, the cerebellar intermediate lobule, as well as the deep cerebellar medial nucleus.

Between-group *t*-tests. To evaluate the directionality (increase or decrease) of group differences in rCBF in brain regions identified by the factorial analysis, we performed between-group Student's *t*-tests at each voxel. Figure 1 reports significant group differences in functional brain activation at $p < 0.05$ for clusters of > 100 contiguous voxels. A summary of the significant group differences pertaining to the basal ganglia-thalamocortical circuit, the cerebellar-thalamocortical circuit and associated motor regions is provided as a diagram in Figure 2.

Lesioned compared to sham-lesioned rats, not surprisingly, showed a significantly decreased rCBF in the motor-sensory cortex (impact site) of the lesioned hemisphere (Fig. 1, Br. 1.0, -1.9 mm) and in ipsilesional dorsal striatum (Fig. 1, Br, 1.0 mm) and the substantia nigra (Fig. 1, -4.8 mm). Significantly decreased rCBF was noted also in the subthalamic nucleus of the lesioned hemisphere. Increased rCBF was noted ipsilesionally in the globus pallidus (external, internal), ventrolateral thalamus, superior colliculus, as well as in the midline central medial nucleus of the thalamus (Fig. 1, Br. -2.4, -6.0 mm). Lesioned compared to sham-lesioned animals showed prominent increases in rCBF in the motor circuit of the nonlesioned hemisphere. Significant increases in rCBF were noted contralateral to the lesion in the classical basal ganglia circuit (anterior motor cortex, dorsal and ventral striatum, external globus pallidus, and ventrolateral thalamus) (Fig. 1, Br. 3.0, 1.0, -1.9, -2.4 mm), as well as in associated motor areas (contralesional red nucleus, pedunculopontine tegmental nucleus, superior colliculus) (Fig. 1, Br. -6.0 mm). Also noted was a significant increase in the rCBF of contralesional sensory cortex (primary somatosensory, primary/secondary visual), as well as the cerebellar vermis, the intermediate cerebellar lobule, and the medial cerebellar nucleus.

Pairwise inter-regional correlation between motor regions. Figure 3 shows the pairwise correlation matrices of the Sham/Saline group and the Lesion/Saline group. A summary of

FIG. 1. Brain regions showing significant between-group differences in *t*-tests. Changes in regional cerebral blood flow-related tissue radioactivity in rats following lesion and physostigmine (PHY) administration. Depicted are representative coronal sections (anterior–posterior coordinates relative to the bregma in millimeters) and top-down view of the cortex. The color-coded statistical parametric maps superimposed on coronal images of the template brain show significant group differences, with *red* and *blue colors* showing positive and negative changes, respectively ($p < 0.05$ at the voxel level for clusters of > 100 contiguous voxels, $n = 9$–14 per group). *White circles* show the approximate location of the right cortical impact injury. Abbreviations: Acb, acumbens nucleus; Au, auditory cortex; CA1, CA3, hippocampus CA1, CA3; Cg1, Cg2, cingulate cortex; CM, central medial thalamus; CPu, striatum; DG, dentate gyrus; LD, lateral dorsal thalamus; GPE, external globus pallidus; GPI, internal globus pallidus; La, lateral amygdala; LO/VO, lateral/ventral orbital frontal cortex; M1, primary motor cortex; M1post, posterior M1; M2, secondary motor cortex; M2post, posterior M2; RPC, red nucleus; S1HL/S1FL/S1Tr/S1BF/S1J, primary somatosensory cortex of the hindlimb/forelimb/trunk/barrelfield/jaw; S2, secondary somatosensory cortex; SC, superior colliculus; Sim, intermediate lobule of the cerebellum; SN, substantia nigra; STN/ZI, subthalamic nucleus-zona incerta; TeA, temporal association cortex; VL, ventrolateral thalamus; VM, ventromedial thalamus; V1, primary visual cortex; V2, secondary visual cortex. Rat brain atlas figures were reproduced from the rat brain atlas,[91] with modification and with permission from Elsevier. Color image is available online at www.liebertpub.com/neu

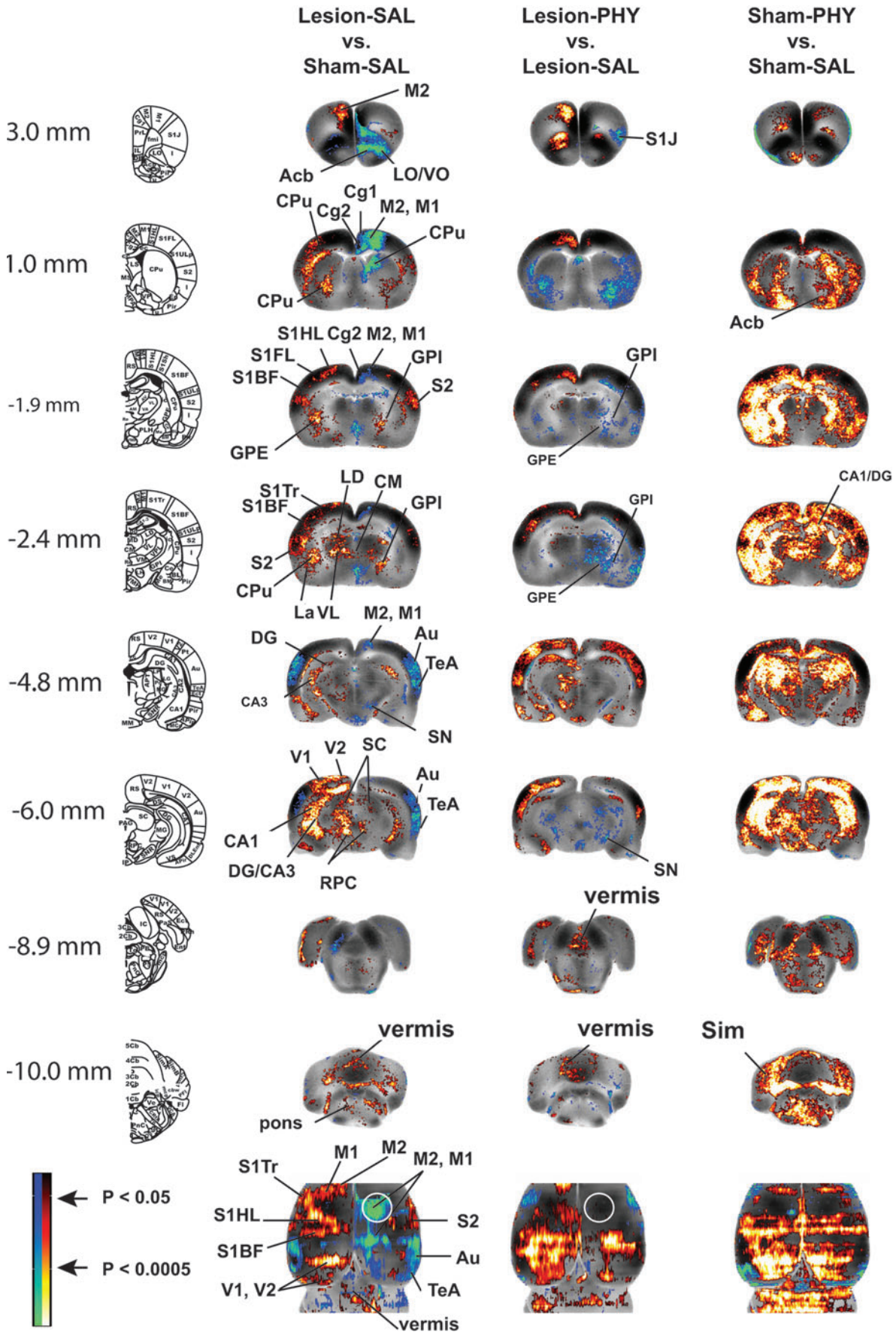
Lesion-SAL vs. Sham-SAL
Lesion-PHY vs. Lesion-SAL
Sham-PHY vs. Sham-SAL
3.0 mm
M2
Acb
LO/VO
S1J
1.0 mm
CPu
Cg1
Cg2
M2, M1
CPu
CPu
Acb
-1.9 mm
S1HL
Cg2
M2, M1
S1FL
S1BF
GPl
S2
GPE
GPl
GPE
-2.4 mm
S1Tr
LD
CM
S1BF
GPl
S2
CPu
La
VL
M2, M1
GPl
GPE
CA1/DG
-4.8 mm
DG
Au
TeA
CA3
SN
-6.0 mm
V1
V2
SC
Au
TeA
CA1
DG/CA3
RPC
SN
-8.9 mm
vermis
-10.0 mm
vermis
pons
vermis
Sim
P < 0.05
P < 0.0005
M1
M2
M2, M1
S1Tr
S1HL
S1BF
V1, V2
S2
Au
TeA
vermis

the number of statistically significant pairwise correlations is provided in Table 2. Lesion/Saline rats compared to Sham/Saline rats showed a net decrease in the total number of pairwise correlations within each of the two hemispheres (intrahemispheric correlations). Decreases were primarily for the negative intrahemispheric correlations, while positive intrahemispheric correlations, in fact, showed a small increase. Significant ipsilesional decreases in functional connectivity (Lesion/Saline vs. Sham/Saline) were noted primarily between motor cortical-to-dorsolateral striatal connections. Significantly increased connectivity was noted ipsilesionally for the globus pallidus (external globus pallidus → primary/secondary motor cortex, dorsolateral striatum; internal globus pallidus → dorsolateral striatum, subthalamic nucleus/zona incerta), the ventrolateral thalamus (ventrolateral thalamus → secondary motor cortex), as well as the superior colliculus (superior colliculus → primary/secondary motor cortex, dorsolateral striatum, substantia nigra), with positive correlations for these structures more limited in the contralesional hemisphere. In addition, there was functional recruitment of the midline cerebellum, which showed significant pairwise correlations primarily for the medial cerebellar nucleus and anterior vermis with the contralesional motor cortex (primary, secondary), while secondary motor cortex additionally showed an increased significant pairwise correlation with the posterior vermis.

Most dramatic was the large decrease in the number of interhemispheric correlations, positive and negative, within the motor circuit (77% decrease in the total number of correlations for the Lesion/Saline compared to the Sham/Saline group). Interhemispheric connectivity was significantly diminished, in particular between motor cortical regions, between the ipsilesional and contralesional dorsolateral striatum, and between the dorsolateral striatum and motor cortex in opposite hemispheres. However, significant increases in interhemispheric connectivity were noted in isolated regions (superior colliculus → primary/secondary motor cortex, subthalamic nucleus/zona incerta; external globus pallidus → dorsolateral striatum, subthalamic nucleus/zona incerta).

Seed analysis in the lesioned brain. Correlation analysis was performed with the contralesional anterior motor cortex as the seed (Fig. 4). Sham lesioned rats administered saline showed a significant positive correlation of the seed with bilateral motor cortex (primary, secondary), with bilateral dorsal striatum, the central medial nucleus of the thalamus and broad areas of contralesional sensory cortex (primary and secondary visual, auditory). Significant bilateral negative correlations were noted with the ventral striatum, red nucleus, substantia nigra, superior colliculus, and pedunculopontine nucleus. Lesioned animals (Lesion/Saline), not unexpectedly, differed from sham-lesioned animals administered saline (Sham/Saline) in that a significant positive correlation of the seed was observed only in contralesional (not bilateral) dorsolateral striatum, and that the bilateral positive correlation with motor cortex was much less broadly represented ipsilesionally. In addition, lesioned compared to sham-lesioned animals showed a broader significant positive correlation with the contralesional sensory cortex (primary somatosensory, temporal association, primary/secondary visual), contralesional subthalamic nucleus/zona incerta, as well as with the midline cerebellar vermis and medial cerebellar nucleus. Correlation ipsilateral to the lesion differed in showing a positive correlation for posterior secondary motor cortex but not primary motor cortex, with significant negative correlations for the striatum and the central medial nucleus. Equivalent results in the Lesion/Saline animals were obtained for the abovementioned brain regions when a correlation analysis was performed with the midline cerebellar vermis as the seed (data not shown).

Effects of physostigmine on motor circuits in the lesioned brain

Factorial analysis. Physostigmine had a differential effect on functional activation of motor regions depending on the presence or absence of the cortical lesion (drug x lesion interaction) (Table 1). Significant changes were noted ipsilesionally in subcortical motor regions, including the dorsolateral striatum, the globus pallidus (external, internal), the thalamus (ventrolateral, ventromedial), and the subthalamic nucleus/zona incerta region. Contralesionally, a significant differential drug x lesion effect was noted only in motor cortex (primary, secondary), in the globus pallidus (external, internal), and in the subthalamic nucleus/zona incerta region. The lesion x drug interaction was also significant in the cerebellar vermis and bilaterally in the intermediate cerebellar lobules.

Between-group *t*-tests. Physostigmine compared to saline-treated lesioned rats showed significantly decreased rCBF broadly in the lesioned hemisphere within the striatum (dorsal and ventral, e.g., Fig. 1, Br. 1.0 mm), globus pallidus (external, internal, Fig. 1 Br. −1.9, −2.4 mm), and substantia nigra (Fig. 1 Br. −6.0 mm), thalamus (ventrolateral, ventromedial, Fig. 1, Br −2.4 mm), and deep white layer of superior colliculus (Fig. 1, Br. −6.0 mm) (for summary, see also Fig. 2). Contralesionally, physostigmine resulted in a significantly increased rCBF in the anterior motor cortex (Fig. 1, Br. 3.0, 1.0, −1.9 mm), subthalamic nucleus/zona incerta (Fig. 1, Br. −4.8 mm), and red nucleus. A significant increase was also noted in the cerebellar vermis (Fig. 1, Br −8.9, −10.0 mm) and bilateral sensory cortex (primary somatosensory, auditory, primary/secondary visual). The physostigmine effect in lesioned animals stands in contrast to that noted in sham-lesioned rats in whom the drug elicited broad, significant bilateral increases in rCBF in the classic basal ganglia circuit, the associated motor regions (superior colliculus, red nucleus, central medial, and ventromedial nuclei of the thalamus, pedunculopontine tegmental nucleus), and the cerebellum.

Pairwise inter-regional correlation in motor circuits of the physostigmine-treated lesioned brain. In lesioned rats, physostigmine compared to saline resulted in a small decrease in the total number of ipsilesional pairwise correlations (intrahemispheric correlations), while the total number of contralesional pairwise correlations remained unchanged (Table 2). Decreases were noted in the positive intrahemispheric correlations, while negative intrahemispheric correlations, in fact, showed a small increase. Also noted was a small increase in significant interhemispheric pairwise correlations, as well as a small increase in the number of pairwise correlation of the cerebellum with other non-cerebellar motor regions. While global connectivity remained largely unchanged by the drug, statistical comparison (Lesion/Phy vs. Lesion/Saline, Fig. 3) showed a modest loss in contralesional pairwise correlations for the motor thalamic regions with the substantia nigra, subthalamic nucleus/zona incerta, and dorsolateral striatum. The effect of physostigmine on increasing the functional connectivity between the anterior cerebellar vermis and contralesional motor cortex and the dorsolateral striatum did not reach statistical significance.

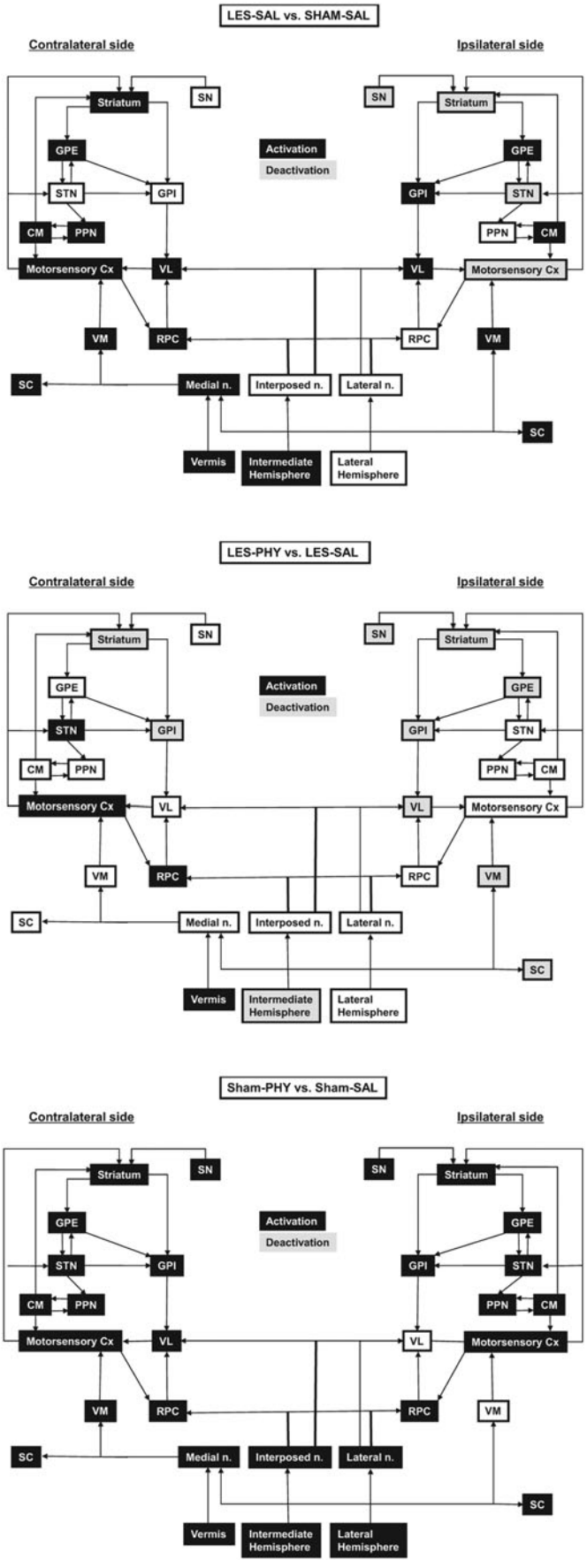

FIG. 2. Summary of the significant changes in functional brain activation **(Top row)** between rats with unilateral motorsensory impact injury and sham-lesioned rats during treadmill walking, as they pertain to the basal ganglia-thalamic-cortical and cerebellar-thalamic-cortical circuits. **(Middle row)** between lesioned rats on chronic physostigmine infusions and lesioned animals administered saline. **(Bottom row)** between sham-lesioned rats on chronic physostigmine and sham-lesioned animals administered saline. *Black shading* indicates a relative increase in regional cerebral perfusion, while *gray* denotes a relative decrease as derived from the SPM maps from Figure 1. Abbreviations: CM, central medial nucleus; GPE, external globus pallidus; GPI, internal globus pallidus; PPN, pedunculopontine tegmental nucleus; RPC, red nucleus; SC, superior colliculus; SN, substantia nigra; STN, subthalamic nucleus; VL, ventrolateral thalamus; VM, ventromedial thalamus. *Arrows* denote known efferent and afferent projections as adapted from Warner (2001)[92] and Wichmann and Dostrowsky (2011).[93]

Seed analysis in the Lesion/Physostigmine animals. Correlation analysis was performed with the contralesional anterior motor cortex as the seed (Fig. 4). Lesioned rats, who were administered physostigmine, different from those administered saline, showed a broad, bilateral, significant positive correlation of the seed, not only with secondary motor cortex, but also with primary motor cortex (Fig. 4, Br. −0.6, −2.4 mm). Lesion/Phy compared to Lesion/Saline rats also showed a broader, significant positive correlation of the seed with sensory cortex (primary/secondary, visual, e.g., Fig. 4, −4.8 mm) and the cerebellar vermis (Fig. 4, Br. −9.7 mm), which was most clearly different ipsilesionally. The positive correlation with contralateral striatum and negative correlation with ipsilesional striatum, while significant, was less broad in the Lesion/Phy versus Lesion/Saline comparison. In addition, physostigmine administration in lesioned rats, different from saline administration, resulted in a new significant positive correlation of the seed with the contralesional ventrolateral thalamus (Fig. 4, −4.8 mm), the central medial nucleus, with significant negative correlations noted bilaterally in the pedunculopontine tegmental nucleus. Equivalent results in the Lesion/Saline and Lesion/Phy animals were obtained for the abovementioned brain regions when a correlation analysis was performed with the cerebellar vermis as the seed (data not shown).

Discussion

Brain regions (motor cortex, basal ganglia, thalamus, and cerebellum) that showed significant differences in functional brain activation after motor cortical impact injury were many of the same brain regions that have previously been reported to be acutely activated/deactivated in normal rats, as investigated during treadmill walking using perfusion–based brain mapping[18] or following microstimulation of the motor cortex using immediate early gene expression (c-fos).[60] Our study is the first to report detailed functional changes that accompany histologic changes within the motor cortex, thalamus, hippocampus, and the cerebellar vermis reported previously by others in the rodent TBI model.[61–63] A central issue highlighted in the current study is that TBI-induced functional changes extend beyond the obvious lesion site to affect remote brain networks. While such diaschisis has been abundantly documented following cerebrovascular stroke,[64] few studies have systematically examined diaschisis after TBI. Prior studies have suggested that focal TBI can result in global changes in excitation and inhibition on the neuronal network level, and that such changes can occur in the absence of histologically significant cell injury.[65] Our study uniquely provides a detailed mapping of the functional reorganization of motor networks occurring after unilateral motor-sensory cortical impact injury.

Cortical impact injury resulted in functional changes in the ipsilesional basal ganglia circuit (indirect and direct pathways), including loss of activation of the motor cortex, striatum, substantia nigra, and subthalamic nucleus, and increased activation of the globus pallidus (external, internal) and ventrolateral thalamus. Functional connectivity was significantly reduced ipsilesionally within motor cortex, and between motor cortex and the striatum. However, increased functional connectivity was noted ipsilesionally between subcortical motor regions, including the superior colliculus, ventrolateral thalamus, globus pallidus (external, internal), possibly as a partial compensation for the cortical injury. Interhemispheric connectivity was greatly diminished, in particular, between motor cortical regions, between the ipsilesional and contralesional dorsolateral striatum, and between the dorsolateral striatum and motor cortex in opposite hemispheres. These findings are consistent with a large number of reports documenting structural abnormalities in transcallosal fibers in TBI subjects.[66–70]

Compensatory changes were noted broadly in the contralesional hemisphere, where we saw significant functional recruitment of stations within the classical basal ganglia circuit, and within associated motor areas (red nucleus, superior colliculus, central medial thalamus, and pedunculopontine tegmental nucleus). Contralesional compensatory changes in the brain are well described in patients following cerebrovascular stroke,[7–9] but have been mostly anecdotally described in TBI subjects. One reason may be that TBI frequently involves widespread brain trauma, and future work will need to examine our findings in blast injury models.

We also noted significant increases in contralesional functional connectivity between the subcortical basal ganglia and motor thalamic regions. Such increases in thalamic functional connectivity are just beginning to be reported in human subjects following TBI.[71] Seed analysis showed that lesioned rats, different from sham-lesioned rats, showed a new significant contralateral functional correlation of motor cortical rCBF with sensory cortical rCBF, suggesting a functional recruitment. Finally, injury resulted in increased rCBF in stations within the contralesional cerebellar–thalamocortical circuit, a circuit that prior work has suggested is capable of motor adaptation and synaptic plasticity (reviewed in Aumann[72]). This picture of broad functional recruitment of the contralesional classical basal ganglia circuit and associated motor regions, limited recruitment of the subcortical motor circuit ipsilesionally, and robust recruitment of regions within the cerebellar–thalamocortical circuit and contralateral sensory cortex was confirmed also by the factorial analysis (Main Effect: Lesion). Whether these changes represent functional recruitment, as has been previously suggested,[73] and/or a reactive change with indirect cell injury after target deprivation remains undetermined.[61–63]

In our prior work, we demonstrated that continuous administration of low dose physostigmine following unilateral motor-sensory impact injury resulted in improved performance on the

FIG. 3. Functional brain connectivity during treadmill walking as displayed using interregional correlation matrices. **(Left column)** Z-scores of Pearson's correlation coefficients are color-coded. The matrix is symmetric across the diagonal line from *upper left to lower right*. Significant correlations ($p < 0.05$) are marked with *white dots*. Cortical impact injury in lesion rats was centered over the right motor-sensory cortex. **(Right column)** The matrix of Fisher's Z-statistics represents differences in Pearson's correlation coefficients (r) between the Lesion/Saline versus the Sham/Saline groups, the Lesion/Phy and Lesion/Saline groups, and the Sham/Phy and Sham/Saline groups. Positive Z values indicate greater r in the Lesion group (or Lesion/Phy group), while negative Z values indicate smaller r. Significant between-group differences ($p < 0.05$) are marked with *white dots*. Abbreviations: dl-CPu, dorsolateral striatum; CM, central medial thalamic n.; GPE, external globus pallidus; GPI, internal globus pallidus; medCb, medial cerebellar n.; M1, primary motor cortex; M1post, posterior M1; M2, secondary motor cortex; M2post, posterior M2; RPC, red nucleus; SC, superior colliculus; SN, substantia nigra; STN/ZI, subthalamic nucleus/zona incerta; antVermis, anterior cerebellar vermis; postVermis, posterior cerebellar vermis; VL, ventrolateral thalamus; VM, ventromedial thalamus. Color image is available online at www.liebertpub.com/neu

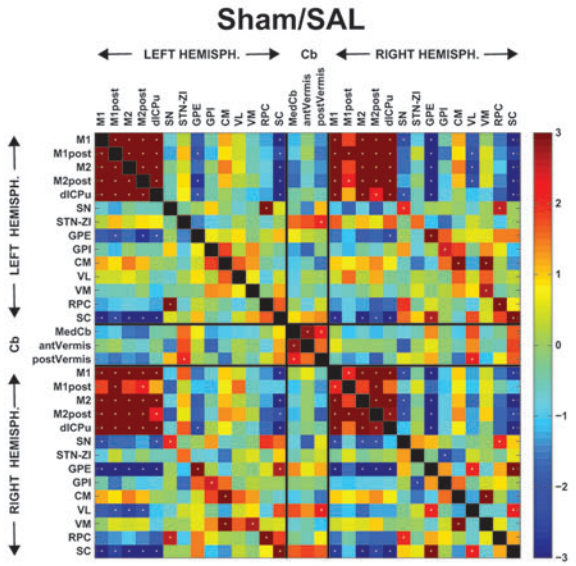
Sham/SAL
LEFT HEMISPH.
Cb
RIGHT HEMISPH.
M1
M1post
M2
M2post
dlCPu
SN
STN-Zl
GPE
GPI
CM
VL
VM
RPC
SC
MedCb
antVermis
postVermis
3
2
1
0
−1
−2
−3

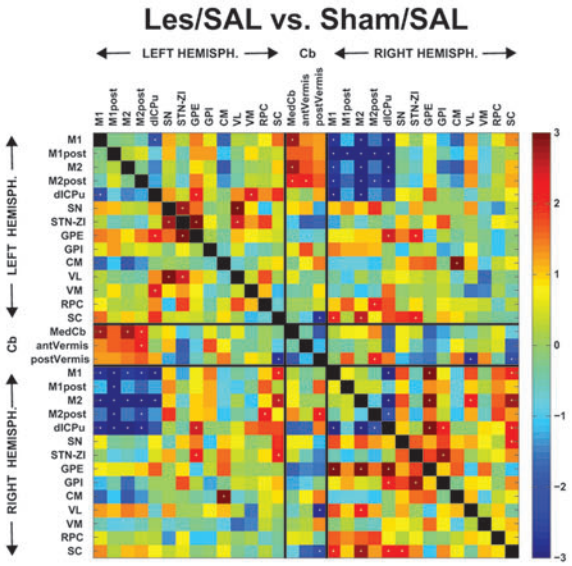
Les/SAL vs. Sham/SAL
LEFT HEMISPH.
Cb
RIGHT HEMISPH.
M1
M1post
M2
M2post
dlCPu
SN
STN-Zl
GPE
GPI
CM
VL
VM
RPC
SC
MedCb
antVermis
postVermis
3
2
1
0
−1
−2
−3

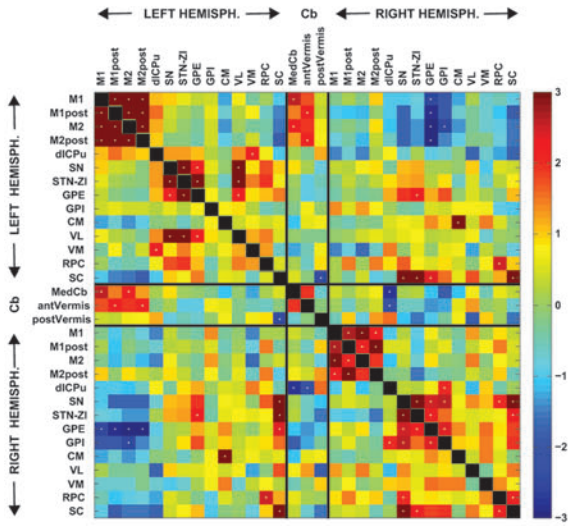
Les/SAL
LEFT HEMISPH.
Cb
RIGHT HEMISPH.
M1
M1post
M2
M2post
dlCPu
SN
STN-Zl
GPE
GPI
CM
VL
VM
RPC
SC
MedCb
antVermis
postVermis
3
2
1
0
−1
−2
−3

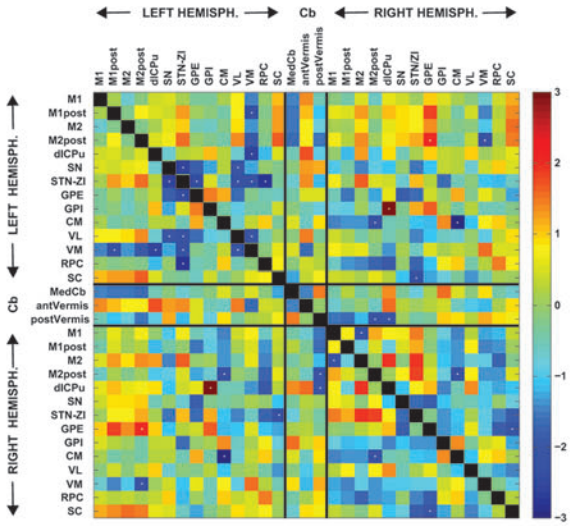
Les/PHY vs. Les/SAL
LEFT HEMISPH.
Cb
RIGHT HEMISPH.
M1
M1post
M2
M2post
dlCPu
SN
STN-Zl
GPE
GPI
CM
VL
VM
RPC
SC
MedCb
antVermis
postVermis
3
2
1
0
−1
−2
−3

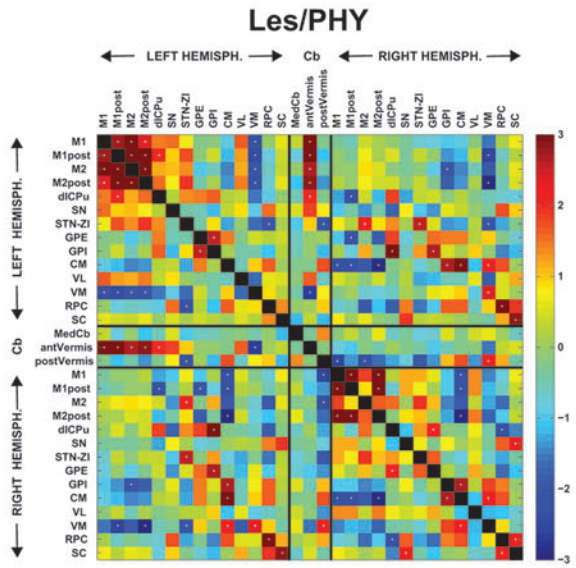
Les/PHY
LEFT HEMISPH.
Cb
RIGHT HEMISPH.
M1
M1post
M2
M2post
dlCPu
SN
STN-Zl
GPE
GPI
CM
VL
VM
RPC
SC
MedCb
antVermis
postVermis
3
2
1
0
−1
−2
−3

Table 2. Pairwise Correlation of rCBF

	Sham/Saline			*Lesion/Saline*			*Lesion/Phy*		
	Pos.	*Neg.*	*Total*	*Pos.*	*Neg.*	*Total*	*Pos.*	*Neg.*	*Total*
Contra	11	8	19	13	0	13	8	5	13
Ipsi	13	12	25	15	0	15	8	4	12
IH	32	20	52	7	5	12	10	9	19
Contra→Cb	1	0	1	4	1	5	5	2	7
Ipsi→Cb	1	0	1	0	2	2	1	2	3

Significant positive (pos.) and negative (neg.) pairwise correlations within the contralesional motor circuit (contra), within the ipsilesional motor circuit (ipsi), and between hemispheres (interhemispheric, IH) after motor cortical impact injury (Lesion/Saline) or sham-injury (Sham/Saline) and in response to physostigmine (Lesion/Phy).

accelerating Rotarod treadmill, with lack of effect or worsening as the dose was increased.[27] In the current study, we showed that effects on functional activation of the lesioned brain after 3 weeks of low dose physostigmine differed between hemispheres. Ipsilateral to the cortical injury, physostigmine compared to saline administration resulted in diminished functional activation of the classic basal ganglia circuit, as well as of the ventromedial thalamus and the superior colliculus. Contralesionally, however, physostigmine increased functional activation of stations within the basal ganglia circuit (motor cortex, subthalamic nucleus) and the red nucleus. Seed analysis showed that Lesion/Phy compared to Lesion/Saline rats also showed also a broader, bilateral, significant positive correlation of motor cortical rCBF with sensory cortical rCBF, suggesting enhanced functional recruitment.

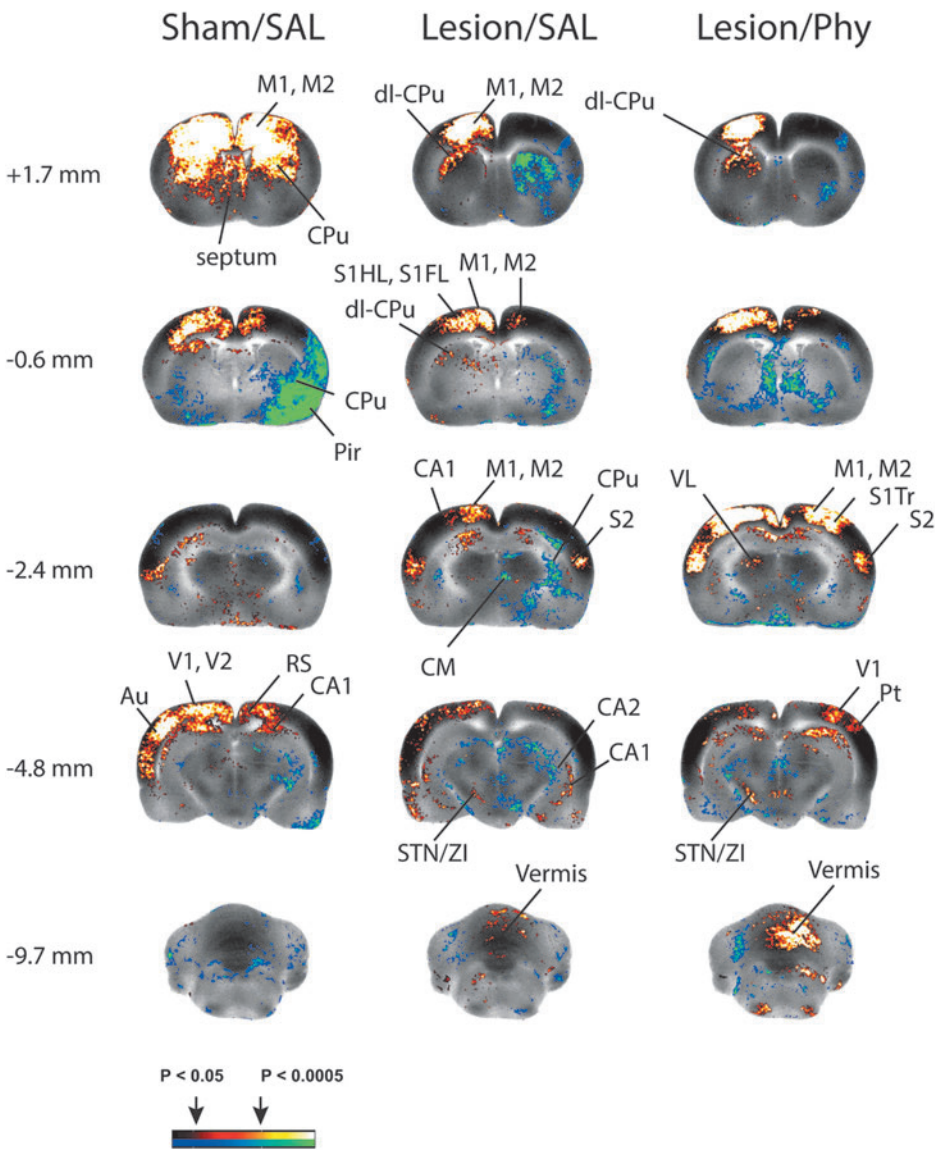

FIG. 4. Correlation of functional brain activation with contralesional anterior motor cortex (left). Shown are significant seed correlations ($p < 0.05$, clusters of > 100 contiguous voxels) with the contralesional anterior motor cortex. Enhanced recruitment of cerebellar-thalamo-cortical circuit and cerebellar-basal ganglia-cortical circuit in response to *right*, unilateral cortical impact injury (Lesion) and of lesioned animals in response to physostigmine administration (Lesion/Phy). Abbreviations: Au, auditory cortex; CA1, CA2, hippocampus CA1, CA2; CPu, striatum; M1, primary motor cortex; M2, secondary motor cortex; dl-CPu, dorsolateral striatum; Pir, piriform cortex; Pt, parietal cortex; S1HL/S1FL/S1Tr, primary somatosensory cortex of the hindlimb/forelimb/trunk; S2, secondary somatosensory cortex; STN/ZI, subthalamic n./zona incerta; VL, ventrolateral thalamus; V1, primary visual cortex; V2, secondary visual cortex. Color image is available online at www.liebertpub.com/neu

Factorial analysis in the current study revealed a drug x lesion interaction for the cerebellar vermis; *t*-tests showed that lesioned rats receiving physostigmine had a greater functional activation of the vermis compared to lesioned rats receiving saline, and seed analysis showed that vermal rCBF was correlated with rCBF within the cerebellar thalamocortical circuit (midline cerebellum → ventrolateral thalamus → motor cortex). Previous autoradiographic, as well as *in situ* hybridization and immunocytochemical studies, have shown that several nicotinic receptor binding sites and subunits are expressed in the adult rat cerebellum. A diffuse cholinergic afferent projection to all lobules of the cerebellar cortex has been described, as well as to the anterior vermis, uvulanodulus, and flocculus regions.[74–76] In addition, cerebellar cholinergic receptors are present in cells within the cerebellum itself.[74–76] Our current results suggest an augmentation of the functional recruitment of the cerebellum by physostigmine. However, such recruitment may remain functionally incomplete, at least at the current dose of the drug. Though pairwise correlation in lesioned rats showed physostigmine to increase the functional connectivity of the vermis to motor cortical regions compared to saline, this trend did not reach statistical significance. Furthermore, while intrahemispheric functional connectivity was largely unchanged ipsilesionally, it showed a few significant decreases between select subcortical motor regions contralaterally.

The current study describes the extensive remote network changes seen after unilateral motor-sensory cortical injury. Such functional reorganization of the brain may augment or impede motor behaviors as has been previously recognized.[8,9] The current study does not directly address this issue. However, if indeed recruitment of the cerebellar–thalamocortical circuit is a compensatory strategy elicited by motor-cortical injury, this would suggest that neurorehabilitation might benefit from incorporation of balance exercise that specifically engages the cerebellum. Preliminary studies suggest modest efficacy of balance training in TBI subjects.[77,78] Similar to our results in the TBI rodent model, earlier work by our group showed hyperactivation of the midline cerebellum during treadmill walking also in rats with unilateral striatal lesions.[79]

Cerebellar hyperactivation can be seen also in subjects with Parkinson's disease,[80–83] an illness that prominently involves the basal ganglia and that shows benefit from balance training.[84,85] Correlation studies have suggested that hyperactivation of the cerebellum and motor cortex represents a compensatory mechanism for hypoactivation in the basal ganglia, rather than a nonspecific pathophysiological response of the disease.[86] Cerebellar hyperactivation in Parkinsonian subjects increases monotonically with increased movement speed of the motor challenge,[80] and shows partial normalization and improvement of motor deficits following levodopa administration.[80,87] Furthermore, bilateral cerebellar transcranial magnetic stimulation in Parkinson's patients induces persistent clinical beneficial effects.[88] These therapeutic changes have been suggested to be mediated by inhibitory Purkinje cells, the output neurons of the cerebellar cortex, which reduce the excitatory drive from the deep cerebellar nuclei via the ventrolateral thalamus to inhibitory neurons in the motor cortex.[89,90] We anticipate that circuit-based approaches into functional brain reorganization will inform future behavioral or molecular strategies to augment targeted neurorehabilitation of TBI patients.

Acknowledgments

This study was supported by a Department of Veterans Affairs Rehabilitation Research & Development Merit Review (VA RR&D) #B5089R and a VA RR&D Research Career Scientist award (OUS).

Author Disclosure Statement

No competing financial interests exist.

References

1. Katz DI, White DK, Alexander MP, and Klein RB. (2004). Recovery of ambulation after traumatic brain injury. Arch Phys Med Rehabil 85, 865–869.
2. Vallee M, McFadyen BJ, Swaine B, Doyon J, Cantin JF, and Dumas D. (2006). Effects of environmental demands on locomotion after traumatic brain injury. Arch Phys Med Rehabil 87, 806–813.
3. Walker GC, Cardenas DD, Guthrie MR, McLean A, Jr, and Brooke MM. (1991). Fatigue and depression in brain-injured patients correlated with quadriceps strength and endurance. Arch Phys Med Rehabil 72, 469–472.
4. Jang SH. (2009). Review of motor recovery in patients with traumatic brain injury. NeuroRehabilitation 24, 349–353.
5. Von Monakow C. (1969). Die Lokalisation im Grosshirn und der Abbau der Funktion durch kortikale Herde (Wiesbaden: Bergmann 1914, tranl. G. Harris). In: *Brain and Behavior I: Mood States and Mind*. Pribam, K.H. (ed). Penguin: Baltimore, MD, pps. 27–36.
6. Carey JR, Kimberley TJ, Lewis SM, Auerbach EJ, Dorsey L, Rundquist P, and Ugurbil K. (2002). Analysis of fMRI and finger tracking training in subjects with chronic stroke. Brain 125, 773–788.
7. Calautti C, Leroy F, Guincestre JY, and Baron JC. (2001). Dynamics of motor network overactivation after striatocapsular stroke: A longitudinal PET study using a fixed-performance paradigm. Stroke 32, 2534–2542.
8. Rehme AK, Fink GR, von Cramon DY, and GrefkesC. (2011). The role of the contralesional motor cortex for motor recovery in the early days after stroke assessed with longitudinal FMRI. Cereb Cortex 21, 756–768.
9. Riecker A, Groschel K, Ackermann H, Schnaudigel S, Kassubek J, and Kastrup A. (2010). The role of the unaffected hemisphere in motor recovery after stroke. Hum Brain Mapp 31, 1017–1029.
10. Rasmussen IA, Xu J, Antonsen IK, et al. (2008). Simple dual tasking recruits prefrontal cortices in chronic severe traumatic brain injury patients, but not in controls. J Neurotrauma 25, 1057–1070.
11. Schallert T, Leasure JL, and Kolb B. (2000). Experience-associated structural events, subependymal cellular proliferative activity, and functional recovery after injury to the central nervous system. J Cereb Blood Flow Metab 20, 1513–1528.
12. Roby-Brami A, Feydy A, Combeaud M, Biryukova EV, Bussel B, and Levin MF. (2003). Motor compensation and recovery for reaching in stroke patients. Acta Neurol Scand 107, 369–381.
13. Jahn K, Deutschlander A, Stephan T, Kalla R, Hufner K, Wagner J, Strupp M, and Brandt T. (2008). Supraspinal locomotor control in quadrupeds and humans. Prog Brain Res 171, 353–362.
14. Hardman CD, Henderson JM, Finkelstein DI, Horne MK, Paxinos G, and Halliday GM. (2002). Comparison of the basal ganglia in rats, marmosets, macaques, baboons, and humans: Volume and neuronal number for the output, internal relay, and striatal modulating nuclei. J Comp Neurol 445, 238–255.
15. Medina L, and Reiner A. (1995). Neurotransmitter organization and connectivity of the basal ganglia in vertebrates: Implications for the evolution of basal ganglia. Brain Behav Evolut 46, 235–258.
16. Smeets WJ, Marin O, and Gonzalez A. (2000). Evolution of the basal ganglia: New perspectives through a comparative approach. J Anat 196, 501–517.
17. Holschneider DP, Maarek JM, Yang J, Harimoto J, and Scremin OU. (2003). Functional brain mapping in freely moving rats during treadmill walking. J Cereb Blood Flow Metab 23, 925–932.
18. Nguyen PT, Holschneider DP, Maarek JM, Yang J, and Mandelkern MA. (2004). Statistical parametric mapping applied to an autoradiographic study of cerebral activation during treadmill walking in rats. Neuroimage 23, 252–259.
19. Fukuyama H, Ouchi Y, Matsuzaki S, et al. (1997). Brain functional activity during gait in normal subjects: A SPECT study. Neurosci Lett 228, 183–186.

20. Hanakawa T, Fukuyama H, Katsumi Y, Honda M, and Shibasaki H. (1999). Enhanced lateral premotor activity during paradoxical gait in Parkinson's disease. Ann Neurol 45, 329–336.
21. Iwaniuk AN, and Whishaw IQ. (2000). On the origin of skilled forelimb movements. Trends Neurosci 23, 372–376.
22. Gharbawie OA, Gonzalez CL, and Whishaw IQ. (2005). Skilled reaching impairments from the lateral frontal cortex component of middle cerebral artery stroke: A qualitative and quantitative comparison to focal motor cortex lesions in rats. Behav Brain Res 156, 125–137.
23. Whishaw IQ, Suchowersky O, Davis L, Sarna J, Metz GA, and Pellis SM. (2002). Impairment of pronation, supination, and body coordination in reach-to-grasp tasks in human Parkinson's disease (PD) reveals homology to deficits in animal models. Behav Brain Res 133, 165–176.
24. Bullmore E, and Sporns O. (2009). Complex brain networks: Graph theoretical analysis of structural and functional systems. Nat Rev Neurosci 10, 186–198.
25. Friston KJ. (1994). Functional and effective connectivity in neuroimaging: A synthesis. Human Brain Map 2, 56.
26. Horwitz B, McIntosh AR, Haxby JV, and Grady CL. (1995). Network analysis of brain cognitive function using metabolic and blood flow data. Behav Brain Res 66, 187–193.
27. Holschneider DP, Guo Y, Roch M, Norman KM, and Scremin OU. (2011). Acetylcholinesterase inhibition and locomotor function after motor-sensory cortex impact injury. J Neurotrauma 28, 1909–1919.
28. Allen AR. (1914). Remarks on the histopathological changes in spinal cord due to impact an experimental study. J Nerv Ment Dis 41, 141–147.
29. Feeney DM, Boyeson MG, Linn RT, Murray HM, and Dail WG. (1981). Responses to cortical injury: I. Methodology and local effects of contusions in the rat. Brain Res 211, 67–77.
30. Scremin OU, Norman KM, Roch M, Holschneider DP, and Scremin AM. (2012). Acetylcholinesterase inhibition interacts with training to reverse spatial learning deficits of cortical impact injury. J Neurotrauma 29, 2457–2364.
31. Scremin OU, Scremin AM, Somani SM, and Giacobini E. (1990). Brain regional distribution of physostigmine and its relation to cerebral blood flow following intravenous administration in rats. J Neurosci Res 26, 188–195.
32. Holschneider DP, Maarek JM, Harimoto J, Yang J, and Scremin OU. (2002). An implantable bolus infusion pump for use in freely moving, nontethered rats. Am J Physiol Heart Circ Physiol 283, H1713–1719.
33. Goldman H, and Sapirstein LA. (1973). Brain blood flow in the conscious and anesthetized rat. Am J Physiol 224, 122–126.
34. Patlak CS, Blasberg RG, and Fenstermacher JD. (1984). An evaluation of errors in the determination of blood flow by the indicator fractionation and tissue equilibration (Kety) methods. J Cereb Blood Flow Metab 4, 47–60.
35. Sakurada O, Kennedy C, Jehle J, Brow, JD, Carbin GL, and Sokoloff L. (1978). Measurement of local cerebral blood flow with iodo [14C] antipyrine. Am J Physiol 234, H59–H66.
36. Jones SC, Korfali E, and Marshall SA. (1991). Cerebral blood flow with the indicator fractionation of [14C]iodoantipyrine: Effect of $PaCO_2$ on cerebral venous appearance time. J Cereb Blood Flow Metab 11, 236–241.
37. Van Uitert RL, and Levy DE. (1978). Regional brain blood flow in the conscious gerbil. Stroke 9, 67–72.
38. Stumpf WE, and Solomon HF. (1995). *Autoradiography and Correlative Imaging.* Academic Press: New York.
39. Thevenaz P, Ruttimann UE, and Unser M. (1998). A pyramid approach to subpixel registration based on intensity. IEEE Trans Image Process 7, 27–41.
40. Brett M, Leff AP, Rorden C, and Ashburner J. (2001). Spatial normalization of brain images with focal lesions using cost function masking. Neuroimage 14, 486–500.
41. Ripolles P, Marco-Pallares J, de Diego-Balaguer R, et al. (2012). Analysis of automated methods for spatial normalization of lesioned brains. Neuroimage 60, 1296–1306.
42. Friston KJ, Holmes A, Worsley KJ, Poline JB, Frith CD, and Frackowiak RS. (1995). Statistical parametric maps in functional imaging: A general linear approach. Human Brain Map 2, 189–210.
43. Friston KJ, Frith CD, Liddle P, Dolan RJ, Lammertsma AA, and Frackowiak RS. (1990). The relationship between global and local changes in PET scans. J Cereb Blood Flow Metab 10, 458–466.
44. Dubois A, Herard AS, Flandin G, et al. (2008). Quantitative validation of voxel-wise statistical analyses of autoradiographic rat brain volumes: Application to unilateral visual stimulation. Neuroimage 40, 482–494.
45. Lee JS, Ahn SH, Lee DS, et al. (2005). Voxel-based statistical analysis of cerebral glucose metabolism in the rat cortical deafness model by 3D reconstruction of brain from autoradiographic images. Eur J Nucl Med Mol Imaging 32, 696–701.
46. Paxinos G, and Watson C. (2005). *The Rat Brain in Stereotactic Coordinates.* 5th edition ed. Elsevier Academic Press: New York, NY.
47. Wang Z, Pang RD, Hernandez M, Ocampo MA, and Holschneider DP. (2012). Anxiolytic-like effect of pregabalin on unconditioned fear in the rat: An autoradiographic brain perfusion mapping and functional connectivity study. Neuroimage 59, 4168–4188.
48. Soncrant TT, Horwitz B, Holloway HW, and Rapoport SI. (1986). The pattern of functional coupling of brain regions in the awake rat. Brain Res 369, 1–11.
49. Nair HP, and Gonzalez-Lima F. (1999). Extinction of behavior in infant rats: Development of functional coupling between septal, hippocampal, and ventral tegmental regions. J Neurosci 19, 8646–8655.
50. Barrett D, Shumake J, Jones D, and Gonzalez-Lima F. (2003). Metabolic mapping of mouse brain activity after extinction of a conditioned emotional response. J Neurosci 23, 5740–5749.
51. Wang Z, Bradesi S, Charles JR, Pang RD, Maarek J-MI, Mayer EA, and Holschneider DP. (2011). Functional brain activation during retrieval of visceral pain-conditioned passive avoidance in the rat. Pain 152, 2746–2756.
52. Shumake J, Conejo-Jimenez N, Gonzalez-Pardo H, and Gonzalez-Lima F. (2004). Brain differences in newborn rats predisposed to helpless and depressive behavior. Brain Res 1030, 267–276.
53. Padilla E, Shumake J, Barrett DW, Sheridan EC, and Gonzalez-Lima F. (2011). Mesolimbic effects of the antidepressant fluoxetine in Holtzman rats, a genetic strain with increased vulnerability to stress. Brain Res 1387, 71–84.
54. Fidalgo C, Conejo NM, Gonzalez-Pardo H, and Arias JL. (2011). Cortico-limbic-striatal contribution after response and reversal learning: A metabolic mapping study. Brain Res 1368, 143–150.
55. Schwarz AJ, Gozzi A, Reese T, and Bifone A. (2007). In vivo mapping of functional connectivity in neurotransmitter systems using pharmacological MRI. Neuroimage 34, 1627–1636.
56. Liang Z, King J, and Zhang N. (2011). Uncovering intrinsic connectional architecture of functional networks in awake rat brain. J Neurosci 31, 3776–3783.
57. Pawela CP, Biswal BB, Cho YR, et al. (2008). Resting-state functional connectivity of the rat brain. Magn Reson Med 59, 1021–1029.
58. Pawela CP, Biswal BB, Hudetz AG, et al. (2010). Interhemispheric neuroplasticity following limb deafferentation detected by resting-state functional connectivity magnetic resonance imaging (fcMRI) and functional magnetic resonance imaging (fMRI). Neuroimage 49, 2467–2478.
59. Magnuson M, Majeed W, and Keilholz SD. (2010). Functional connectivity in blood oxygenation level-dependent and cerebral blood volume-weighted resting state functional magnetic resonance imaging in the rat brain. J Magn Reson Imag 32, 584–592.
60. Wan XS, Liang F, Moret V, Wiesendanger M, and Rouiller EM. (1992). Mapping of the motor pathways in rats: C-fos induction by intracortical microstimulation of the motor cortex correlated with efferent connectivity of the site of cortical stimulation. Neuroscience 49, 749–761.
61. Conti AC, Raghupathi R, Trojanowski JQ, and McIntosh TK. (1998). Experimental brain injury induces regionally distinct apoptosis during the acute and delayed post-traumatic period. J Neurosci 18, 5663–5672.
62. Matthews MA, Carey ME, Soblosky JS, Davidson JF, and Tabor SL. (1998). Focal brain injury and its effects on cerebral mantle, neurons, and fiber tracks. Brain Res 794, 1–18.
63. Sato M, Chang E, Igarashi T, and Noble LJ. (2001). Neuronal injury and loss after traumatic brain injury: Time course and regional variability. Brain Res 917, 45–54.
64. Mountz JM. (2007). Nuclear medicine in the rehabilitative treatment evaluation in stroke recovery. Role of diaschisis resolution and cerebral reorganization. Eur Medicophys 43, 221–239.
65. Ding MC, Wang Q, Lo EH, and Stanley GB. (2011). Cortical excitation and inhibition following focal traumatic brain injury. J Neurosci 31, 14085–14094.

66. Caeyenberghs K, Leemans A, Coxon J, et al. (2011). Bimanual coordination and corpus callosum microstructure in young adults with traumatic brain injury: A diffusion tensor imaging study. J Neurotrauma 28, 897–913.
67. Farbota KD, Bendlin BB, Alexander AL, Rowley HA, Dempsey RJ, and Johnson SC. (2012). Longitudinal diffusion tensor imaging and neuropsychological correlates in traumatic brain injury patients. Frontiers Human Neurosci 6, 160.
68. Niogi SN, Mukherjee P, Ghajar J, et al. (2008). Extent of microstructural white matter injury in postconcussive syndrome correlates with impaired cognitive reaction time: A 3T diffusion tensor imaging study of mild traumatic brain injury. AJNR. Am J Neuroradiol 29, 967–973.
69. Palacios EM, Fernandez-Espejo D, Junque C, et al. (2011). Diffusion tensor imaging differences relate to memory deficits in diffuse traumatic brain injury. BMC Neurol 11, 24.
70. Wu TC, Wilde EA, Bigler ED, et al. (2010). Longitudinal changes in the corpus callosum following pediatric traumatic brain injury. Develop Neurosci 32, 361–373.
71. Tang L, Ge Y, Sodickson DK, Miles L, Zhou Y, Reaume J, and Grossman RI. (2011). Thalamic resting-state functional networks: Disruption in patients with mild traumatic brain injury. Radiology 260, 831–840.
72. Aumann TD. (2002). Cerebello-thalamic synapses and motor adaptation. Cerebellum 1, 69–77.
73. Lewis DH, Bluestone JP, Savina M, Zoller WH, Meshberg EB, and Minoshima S. (2006). Imaging cerebral activity in recovery from chronic traumatic brain injury: A preliminary report. J Neuroimag 16, 272–277.
74. De Filippi G, Baldwinson T, and Sher E. (2005). Nicotinic receptor modulation of neurotransmitter release in the cerebellum. Prog Brain Res 148, 307–320.
75. Oki T, Takagi Y, Inagaki S, Taketo MM, Manabe T, Matsui M, and Yamada S. (2005). Quantitative analysis of binding parameters of [3H]N-methylscopolamine in central nervous system of muscarinic acetylcholine receptor knockout mice. Mol Brain Res 133, 6–11.
76. Turner JR, Ortinski PI, Sherrard RM, and Kellar KJ. (2011). Cerebellar nicotinic cholinergic receptors are intrinsic to the cerebellum: Implications for diverse functional roles. Cerebellum 10, 748–757.
77. Dault MC, and Dugas C. (2002). Evaluation of a specific balance and coordination programme for individuals with a traumatic brain injury. Brain Inj 16, 231–244.
78. Katz-Leurer M, Rotem H, Keren O, and Meyer S. (2010). Recreational physical activities among children with a history of severe traumatic brain injury. Brain Inj 24, 1561–1567.
79. Yang J, Sadler TR, Givrad TK, Maarek JM, and Holschneider DP. (2007). Changes in brain functional activation during resting and locomotor states after unilateral nigrostriatal damage in rats. Neuroimage 36, 755–773.
80. Palmer SJ, Ng B, Abugharbieh R, Eigenraam L, and McKeown MJ. (2009). Motor reserve and novel area recruitment: Amplitude and spatial characteristics of compensation in Parkinson's disease. Eur J Neurosci 29, 2187–2196.
81. Ballanger B, Baraduc P, Broussolle E, Le Bars D, Desmurget M, and Thobois S. (2008). Motor urgency is mediated by the contralateral cerebellum in Parkinson's disease. J Neurol Neurosurg Psychiatry 79, 1110–1116.
82. Wu T, and Hallett M. (2008). Neural correlates of dual task performance in patients with Parkinson's disease. J Neurol Neurosurg Psychiatry 79, 760–766.
83. Cerasa A, Hagberg GE, Peppe A, et al. (2006). Functional changes in the activity of cerebellum and frontostriatal regions during externally and internally timed movement in Parkinson's disease. Brain Res Bull 71, 259–269.
84. Keus SH, Bloem BR, Hendriks EJ, Bredero-Cohen AB, Munneke M, and Practice Recommendations Development, G. (2007). Evidence-based analysis of physical therapy in Parkinson's disease with recommendations for practice and research. Movement Dis 22, 451–460; quiz 600.
85. Esculier JF, Vaudrin J, Beriault P, Gagnon K, and Tremblay LE. (2012). Home-based balance training programme using Wii Fit with balance board for Parkinsons's disease: A pilot study. J Rehab Med 44, 144–150.
86. Yu, H., Sternad, D., Corcos, D.M. and Vaillancourt, D.E. (2007). Role of hyperactive cerebellum and motor cortex in Parkinson's disease. Neuroimage 35, 222–233.
87. Wu T, Wang L, Chen Y, Zhao C, Li K, and Chan P. (2009). Changes of functional connectivity of the motor network in the resting state in Parkinson's disease. Neurosci Lett 460, 6–10.
88. Koch G, Brusa L, Carrillo F, et al. (2009). Cerebellar magnetic stimulation decreases levodopa-induced dyskinesias in Parkinson disease. Neurology 73, 113–119.
89. Langguth B, Eichhammer P, Zowe M, et al. (2008). Modulating cerebello-thalamocortical pathways by neuronavigated cerebellar repetitive transcranial stimulation (rTMS). Neurophysiol Clin 38, 289–295.
90. Na J, Kakei S, and Shinoda Y. (1997). Cerebellar input to corticothalamic neurons in layers V and VI in the motor cortex. Neurosci Res 28, 77–91.
91. Paxinos G, and Watson C. (2007). *The Rat Brain in Stereotactic Coordinates.* 6th ed. Elsevier Academic Press: New York.
92. Warner JJ. (2001). *Atlas of Neuroanatomy with Systems Organization and Case Correlations.* Butterworth Heinemann: Boston.
93. Wichmann T, and Dostrovsky JO. (2011). Pathological basal ganglia activity in movement disorders. Neuroscience 198, 232–244.

Address correspondence to:
Daniel P. Holschneider, MD
Department of Psychiatry and Behavioral Sciences
University of Southern California
1333 San Pablo Street, MCH-51A, MC9151
Los Angeles, CA 90033

E-mail: holschne@usc.edu